BULETINUL INSTITUTULUI POLITEHNIC DIN IAŞI
(BULLETIN OF THE POLYTECHNIC INSTITUTE OF IAŞI)
Published by "Gheorghe Asachi" Technical University of Iaşi
Section Mathematics. Theoretical Mechanics. Physics

Volume 68(72), No. 1, 2022
DOI: 10.2478/bipmf-2022-0002

RESEARCH ON OBTAINING AND CHARACTERIZING NI - W ELECTROPLATING ALLOYS FOR MICRO-ELECTRO MECHANICS

MARIA POROCH – SERIȚAN [1], IGOR CREȚESCU [2], GHEORGHE GUTT [1], MARIUS PRELIPCEANU [3], RADU FECHET [3], DRAGOŞ VICOVEANU [3], OTILIA – SANDA PRELIPCEANU [4, *] and ANDREI POROCH – SERIȚAN [3]

[1]*Faculty of Food Engineering, "Stefan cel Mare" University of Suceava, 13 Universitatii Street, 720229, Suceava, Romania*
[2]*Faculty of Chemical Engineering and Environmental Protection, "Gheorghe Asachi" Technical University of Iaşi, 73 D. Mangeron Street, 700050, Iaşi, Romania*
[3]*Faculty of Electrical Engineering and Computer Science, "Stefan cel Mare" University of Suceava, 13 Universitatii Street, 720229, Suceava, Romania*
[4]*Faculty of Physics "Alexandru Ioan Cuza" University of Iaşi, 11 Boulevard Carol I, 700506, Iaşi, Romania*
**Corresponding author e-mail: marius.prelipceanu@usm.ro*

Citation:

POROCH - SERIȚAN MARIA, CREȚESCU IGOR, GUTT GHEORGHE, PRELIPCEANU MARIUS, FECHET RADU, VICOVEANU DRAGOŞ, PRELIPCEANU OTILIA - SANDA and POROCH – SERIȚAN ANDREI;

RESEARCH ON OBTAINING AND CHARACTERIZING NI - W ELECTROPLATING ALLOYS FOR MICRO-ELECTRO MECHANICS;

BULLETIN OF THE POLYTECHNIC INSTITUTE OF IAȘI, 2022, 68(72), 1, 21-34;

DOI: 10.2478/bipmf-2022-0002.

Received: January 20, 2022
Accepted: March 15, 2022
Publication: March 30, 2022

© 2022 Poroch - Seriţan M. *et al.*

This is an Open access article licensed under the Creative Commons Attribution-NonCommercial – NoDericatives 4.0 International License (CC BY-NV-ND 4.0)

Abstract. The present research aimed to electrodeposit and characterize Ni-W alloys for different technological parameters, being an example of "induced co-deposition", in which a certain metal (for example: Mo, W) can be co-deposited as an alloy, but it cannot be measured in its pure state. The investigated characteristics were the efficiency current, the average thickness, and the structural properties of the obtained deposits. The current efficiency decreases with an increased applied current density, and the tungsten content remains constant at around 11% for different current densities (10 mA·cm^{-2} and 16 mA·cm^{-2}, respectively). An increase in the temperature of the electrolyte leads to the inclusion of more tungsten. The deposit tungsten content and the current efficiency are directly related to pH. The deposit hardness directly relates to the alloy composition, deposit morphology, and coating thickness. The higher hardness, approximatively 100 HV were measured and the optimal brightness were observed for the alloys obtained at increased current density (i = 16 mA·cm^{-2}, T = 50°C, pH = 8), or to a basic pH (i = 10 mA·cm^{-2}, T = 50°C, pH = 9.23). The scanning electron microscopy (SEM) technique was used to analyze the surface morphology, and energy dispersive spectroscopy (EDS) analysis was carried out to determine the composition of the alloys. The metallic surface brightness (%) was evaluated using the miniature spectrometer, based on the reflection property of the electrodeposited metallic layer, scanning the all-wavelength range between 200-1100 nm.

Keywords: current density, temperature, pH. hardness, deposit morphology

1. Introduction

Ni - W electroplating alloys have found a wide range of applications in engineering due to their excellent properties of corrosion and wear resistance and mainly due to their unique combination of tribological, magnetic, electrical, and electro-erosion properties [1-5], These have good mechanical properties (i.e., high tensile strength and first hardness on the hardness scale, superior abrasion resistance, corrosion resistance), excellent resistance to strong oxidizing acids, and high melting temperatures [6-9]. In the field of micromechanical technologies, due to rapid developments, the demand for exceptional mechanical and physical properties continues to grow, and therefore Ni-W alloys are a perfect choice in the production of microelectromechanical structures and microdevices [10, 11]. The Ni - W alloy system is known for the expected electrolytic properties of electrodes that improve the current and energy efficiency of the hydrogen evolution reaction (HER) from alkaline solutions [12-25].

Our research focused on the study of the properties of NiW electrodeposits from a structural point of view by energy dispersive spectroscopy (EDS), morphologically by scanning electron microscopy (SEM) and atomic force spectroscopy (AFM); and hardness to obtain alloys for micro-electro mechanics in optimal conditions with the most efficient yield and the desired properties.

2. Materials and Methods

The composition of the electrolytes used to obtain the electrochemical deposits of Ni - W alloys are: nickel sulfate hexahydrate 26.29 [g·L^{-1}]; sodium tungstate dihydrate 131.94 [g·L^{-1}]; tri-sodium citrate dihydrate 147 [g·L^{-1}] [7-9, 26]. For the Ni-W coatings, electrolytic copper flat plates with a purity of 99.98% were employed as cathodes, figure 1. The anode used for Ni-W alloy deposition is an insoluble spectral graphite anode with an anode-to-cathode area ratio is 1:10.

The cathodic current efficiency in the electrodeposition of Ni-W alloys was calculated according to the following equation:

$$\eta = \frac{(m \cdot Ni\%)/Eq_1 + (m \cdot W\%)/Eq_2}{I \cdot t} \quad (1)$$

where:

m is the weight of the deposit [g], *Ni*% and *W*% [wt%] is the percentage of nickel and tungsten in the deposits, Eq_1 and Eq_2 are the electrochemical equivalents of the ions of [Ni2+] and [W6+] [g/C], I is the deposition current [A] and t is the deposition time [s].

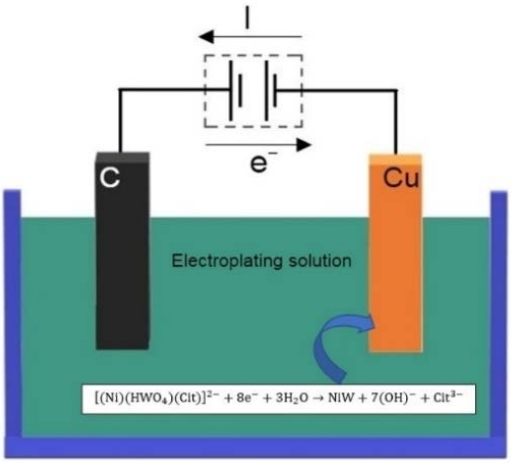


Fig. 1 − Electroplating cell

The composition of the deposits was determined using the EDS (Bruker AXS Microanalysis GmbH probe) attached to a SEM (VEGA II LMU - Tescan, Czech Republic). The average thickness of the alloy layer was calculated by measuring seven local values of cathode thickness after electro-deposition and taking the initial thickness as reference. The measurements of the thickness mentioned above were carried out using a PosiTector 6000 - DeFesko Analyser, based on a non-destructive physical method [27].

The micro-hardness [HV] of the metallic cover was measured using the Shimadzu HMV – 2T micro-hardness analyser. The loading weight was 490.3 mN, and the load duration was 15 s, respectively [27, 28]. The roughness measurement of the surfaces of the deposited layers was performed by a 3D Profilometer - system µScan (NanoFocus AG µScan). The scanned surfaces were 1 mm x 1 mm, at a resolution of 2 µm x 2 µm (500 x 500 points).

The brightness of the metallic cover, [%], was carried out using the HR 4000 CG-UV-NIR, Ocean Optics Inc., Dunedin, FL, a miniature spectrometer based on the reflection property of the electrodeposited metallic layer [27].

The structure analysis of the deposits to characterize the structure type and the orientation of the crystals in the layer was performed by X-ray diffraction in the configuration θ - 2θ, with a diffractometer Bruker AXS model D8 Discover. The X-ray tube emits CuKα radiation, which uses the wavelength, λ = 1.54184 Å. The analysis studies of the structure of the deposited layer and the topography of the sample were completed by the AFM studies performed with the scanning probe microscope. (SPM) - (Scanning Probe Microscope – SOLVER) [27].

Table 1 shows the correspondence between the real and coded values of variables by the process (current density [mA·cm^{-2}], temperature [ºC], solution pH) because current density [mA·cm^{-2}], temperature [ºC], solution pH are the main factors that influence the electrodeposition of the Ni-W alloy. By programming the experiment in the factorial space, we went from the real values of the influencing factors to equivalent codified values. Thus, the higher level of each factor was coded with = + 1, the lower level with = - 1, and the base level with = 0. The information regarding the variation limits of the variables of the electrodeposition process, as well as the correlation between the actual values and the levels of coding are presented in table 1. The planning of the experiment was carried out in accordance with a central - compositional - orthogonal program of order two.

Table 1. Correspondence between the real and coded values of variables by the process

Variables of process (factors)	Coded variables	Real values of coded levels					Range of variations
		$-\alpha$	- 1	0	+ 1	$+\alpha$	
i, current density [mA·cm^{-2}]	x_1	3.875	5	10	15	16.125	5
T, temperature [ºC]	x_2	25.5	30	50	70	74.5	20
solution *pH*	x_3	6.775	7.00	8	9.00	9.225	1

3. Result and discussions

In industrial practice it is well known that the electrodeposition of nickel and tungsten is very sensitive to changes in working conditions. The influence of technological parameters (current density, temperature and pH) on the electrochemically obtained Ni-W alloy deposits from a citrate-based bath was studied. Table 2 shows the responses (cathodic current efficiency [%], thickness layer [µm], roughness [µm], brightness [%]) of the electrodeposition system to the parameters required by the process.

The electrodeposition of Ni-W alloys on the metals is possible in theory when an appropriate complex agent and certain plating conditions are selected during the "induced co-deposition" process. This process has been extensively analysed due to the variety of high-tech applications viewed in terms of their broad spectrum of physical properties, and numerous models have been

Table 2. Matrix of orthogonal central composite programming of second order and responses

No. sample	Electroplating parameters			Responses (performance criteria)				
	***i*, [mA·cm^{-2}]**	***T*, [ºC]**	**pH**	**Cathodic current efficiency [%]**	**Thickness layer [µm]**	**Hardness [HV]**	**Roughness [µm]**	**Brightness [%]**
1	-1	-1	-1	1.231	0.500	100.0	Sa = 0.749 Sq = 0.948	14.724
2	1	-1	-1	4.163	1.333	98.6	Sa = 0.698 Sq = 0.901	11.067
3	-1	1	-1	10.630	0.666	106.7	Sa = 0.698 Sq = 0.901	4.780
4	1	1	-1	4.853	1.666	102.7	Sa = 0.643 Sq = 0.821	7.387
5	-1	-1	1	0.164	0.833	92.6	Sa = 0.710 Sq = 0.916	19.134
6	1	-1	1	0.069	0.666	95.1	Sa = 0.685 Sq = 0.872	14.126
7	-1	1	1	6.345	1.333	95.4	Sa = 0.677 Sq = 0.877	22.835
8	1	1	1	1.972	0.833	99.7	Sa = 0.849 Sq = 1.092	16.038
9	$+\alpha$	0	0	1.774	0.666	99.5	Sa = 0.707 Sq = 0.902	11.212
10	$-\alpha$	0	0	4.951	0.833	103.0	Sa = 0.593 Sq = 0.771	10.018

11	0	+ α	0	5.893	0.666	112.0	Sa = 0.594 Sq = 0.761	7.434
12	0	- α	0	0.557	1.166	93.8	Sa = 0.801 Sq = 1.049	10.464
13	0	0	+ α	0.424	0.833	98.0	Sa = 0.801 Sq = 1.049	20.841
14	0	0	- α	2.894	1.000	99.0	Sa = 0.789 Sq = 1.045	14.204
15	0	0	0	3.307	1.000	100.5	Sa = 0.650 Sq = 0.831	13.994
16	0	0	0	2.336	1.166	96.0	Sa = 0.928 Sq = 1.158	11.046
Sa = (the arithmetic mean of the absolute departures of the roughness profile from the mean line throughout the sampling length) Sq = (the root mean square deviation of the assessed profile)								

developed for predicting this behaviour [4, 29-52]. However, although several models have been proposed, the "induced co-deposition" mechanism is not fully understood. The general reaction of the ternary complex requires eight electrons and can be written according to eq. 2:

$$\left[(Ni)(HWO_4)(Cit)\right]^{2-} + 8e^- + 3H_2O \rightarrow NiW + 7(OH)^- + Cit^{3-} \quad (2)$$

In most cases, the cathodic current efficiency of Ni-W alloys co-deposited in citrate-based baths is much lower than 100%, which denotes the simultaneous release of hydrogen in large quantities. It should be noted that Ni-W co-deposition is complicated by the simultaneous discharge of hydrogen ions, which occurs both during the separate electrodeposition of nickel and during the co-deposition of Ni-W alloy [53].

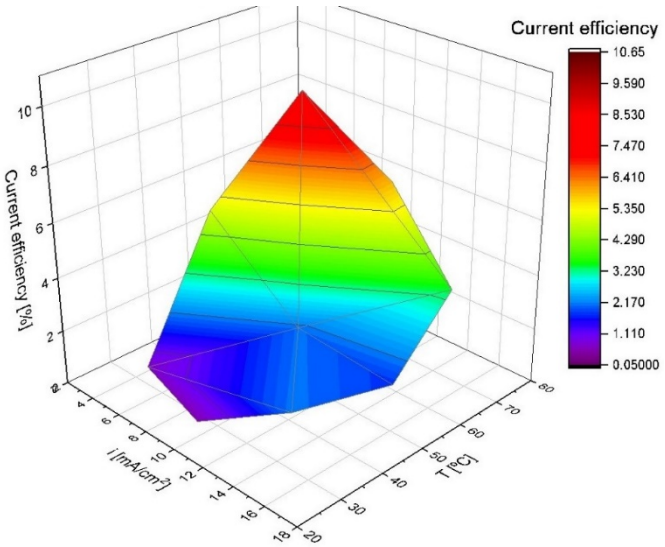


Fig. 2 − The cathodic current efficiency profile in respect with current density and temperature

The current efficiency decreased as the current density increased, figure 2, and the tungsten content remained constant at around 11% W for the current densities of 10 mA·cm^{-2} and 16 mA·cm^{-2}, respectively. At high current densities, at which the current yield is low, the release of hydrogen

becomes more prominent and causes further stirring of the solution. Moreover, because Ni is easily deposited compared to W, it is expected that the high current yield will cause a higher concentration of Ni. However, these results indicate some degree of limitation of mass transport. The pH of the bath has an important effect on the current efficiency as well as on the tungsten content in the deposit. Increasing the pH from 6.78 to 8 increases the tungsten content from 13.51% to 14.65% and at the same time increases the current efficiency, figure 2. A further increase in pH from 8 to 9.23 causes a decrease in both the current yield and the tungsten and nickel content, respectively. The respective tungsten nickel content as well as the current efficiency increase with increasing temperature, figure 2. The increasing behaviour of the tungsten content with the increase of the bath temperature in both non-stirred and stirred baths was explained in terms of favourable conditions for the transport of tungsten to the cathode surface. It has also been found that the deposition rate increases with increasing temperature in the 50 – 74.5°C range.

AFM images purchased in the contact module, in air, recorded on an area of 10 µm x 10 µm electrodeposited Ni-W alloys, at various parameters are shown in the figure 3, figure 4, figure 5. The surface of the Ni - W alloy layer electrodeposited at pH = 7, at i = 15.00 mA·cm^{-2}, T = 30°C is seen in figure 3. The size and width of the grains vary over the entire surface. The three-dimensional image seen in figure 3b reveals a relatively homogeneous coverage. The dark areas in Figure 3a represent the substrate, and the light areas represent the deposited layer. When the current density decreased and the electrolyte temperature and pH were increased (i = 5.00 mA·cm-2, T = 70°C, pH = 9), the surface of the layer led to a smaller size of the Ni -W alloy coating granules, as shown in Figure 4. The AFM image clearly shows that the Ni - W beams still vary in size and shape.

At i = 10.00 mA·cm^{-2}, T = 25.5°C, pH = 8, a reduction of the granule size can be observed in the Ni - W coatings compared to i = 15.00 mA·cm-2, T = 30°C, pH = 7. The three-dimensional AFM image (Figure 5b) shows the small overall grain size and surface morphology of this coating. The comparison of this deposit with the previous coatings shows that the Ni-W grains are lower at pH 8, with a rough but uniform appearance, which is consistent with images obtained with profilometer, figure 12.

The experimental results indicate that the size of the granules increases with increasing current density and temperature. Moreover, the high temperature favours deposits in the same direction and homogeneous. The three-dimensional image seen in figure 3b shows that the height of the individual grains varies and the largest grains seen in the deposit are 0.32 µm above the surface.

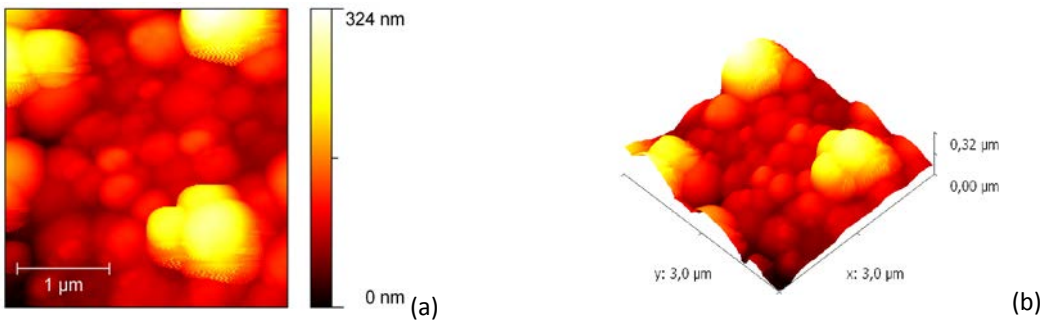


Fig. 3 − AFM images of NiW electrodeposition on copper substrate obtained at *i* = 15.00 mA·cm^{-2}, T = 30°C, pH = 7 (no sample 2)

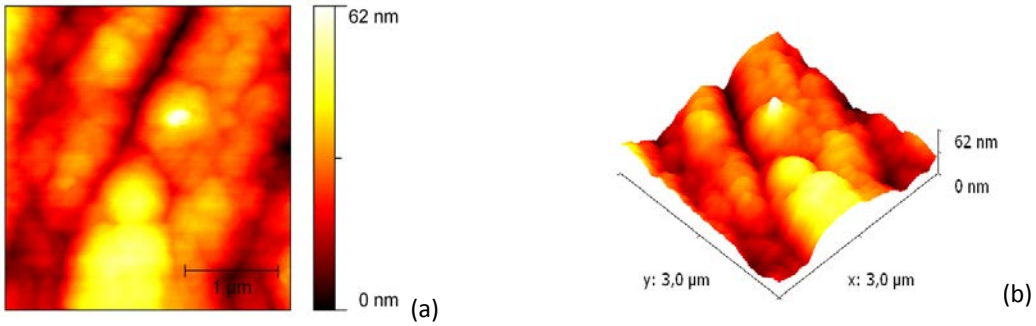


Fig. 4 − AFM images of NiW electrodeposition on copper substrate obtained at i = 5.00 mA·cm^{-2}, T = 70°C, pH = 9 (no sample 7)

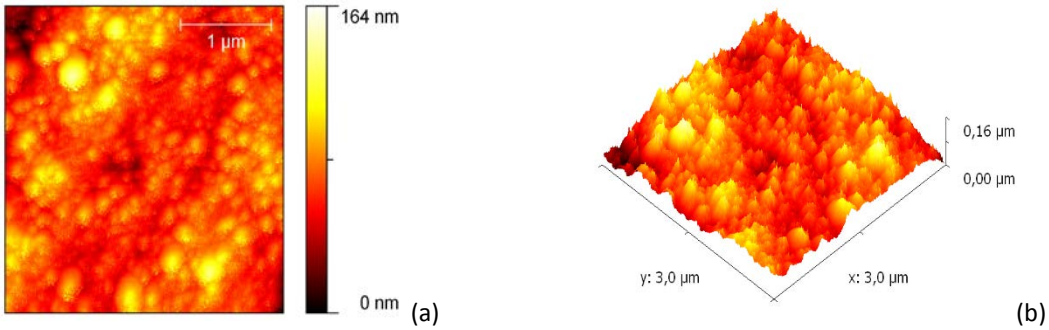
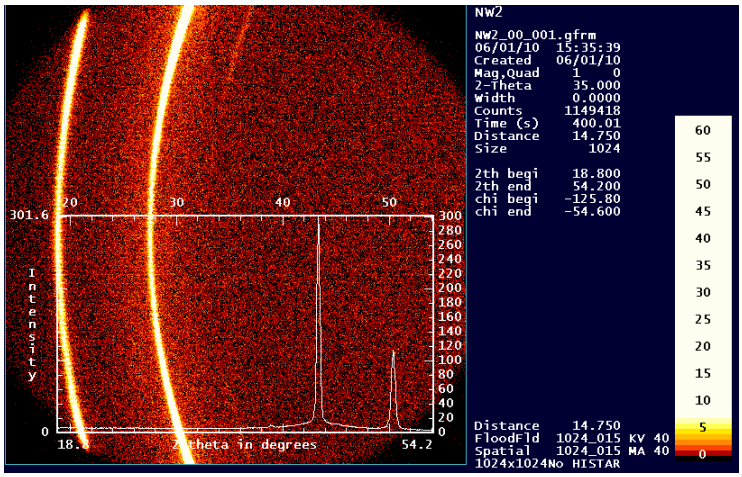


Fig. 5 − AFM images of NiW electrodeposition on copper substrate obtained at i = 10.00 mA·cm^{-2}, T = 25.5°C, pH = 8 (no sample 12)

Diffractogram of a Ni-W alloy deposit deposited on a copper substrate at pH = 7, i = 15.00 mA·cm^{-2} and T = 30°C and the representation of the intensity as a function of 2θ by integrating the data from the diffractogram are represented in the figure 6.



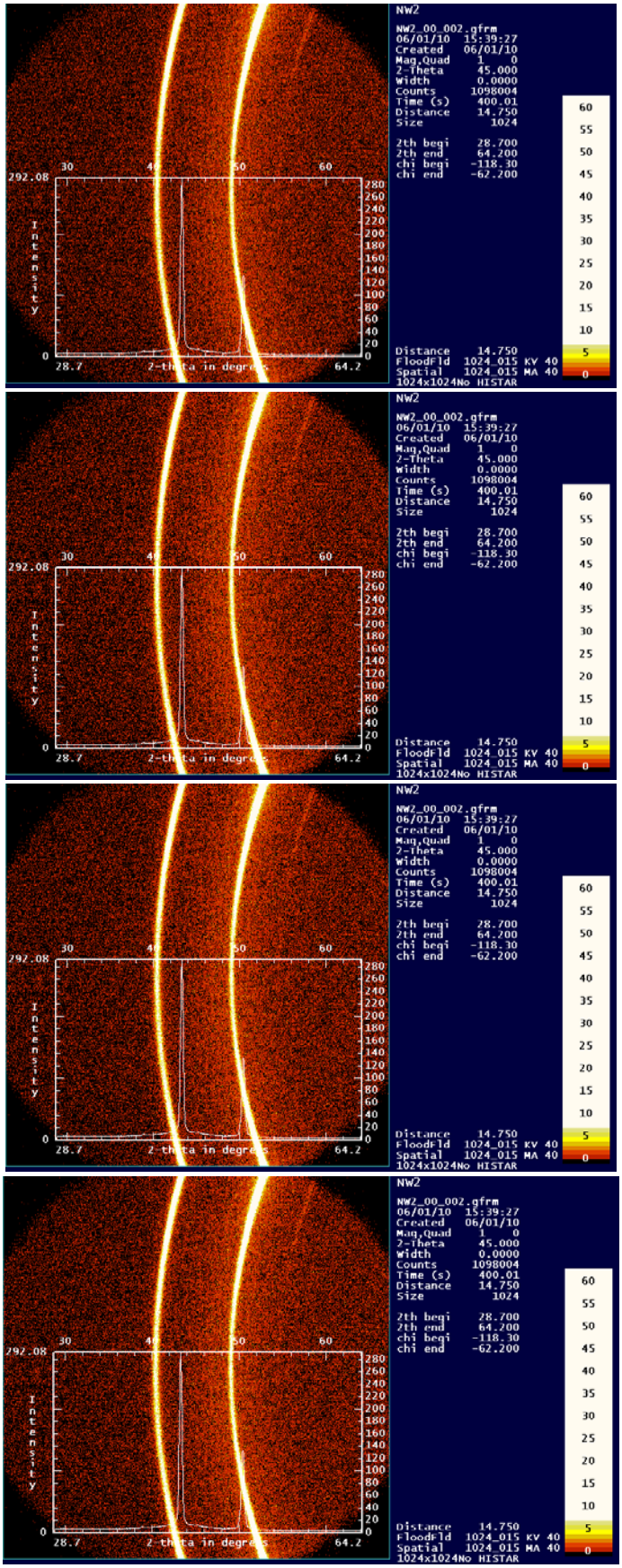


Fig. 6 − Debye Scherrer diagram of NiW electrodeposition on copper substrate obtained at i = 15.00 mA·cm^{-2}, T = 30°C, pH = 7, for 15.5 min. (no sample 2)

The patterns exhibit a small shoulder at 2θ = 42º corresponding to the Ni-W alloy [55, 56]. The microstructure of the Ni-W deposits exhibits (111) preferred orientation similar to the fcc (111) phase of Ni. Changing the operating conditions has no significant effect on the XRD patterns [54]; some authors [55, 56] have reported the formation of amorphous Ni-W alloys. However, the data shown here cannot be taken as evidence that amorphous alloys have also been deposited. The noncrystalline alloy structure must arise because the deposition process produces mutually incoherent particles which are too small for the crystalline configuration to be formed energetically [57] or because the atoms do not bond together in the arrangement required for crystalline long-range order [56].

Depending on the electrolysis parameters, the properties of the alloy deposits vary: layer thickness, hardness and brightness. The highest layer thickness of the analysed deposits was obtained under the following electrodeposition conditions: i = 10 mA·cm^{-2}, T = 50°C, pH = 8, without stirring.

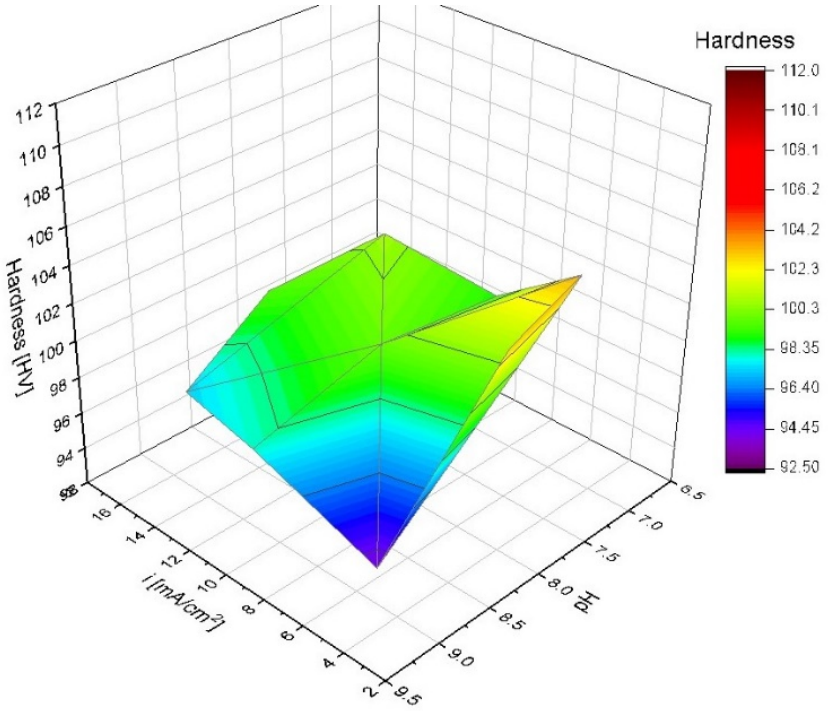


Fig. 7 − The hardness profile as a function of current density and pH

The hardness of the deposits is influenced by the composition of the alloy, by the phases that enter the morphology of the deposit, as well as by the thickness of the deposited layer. The highest hardness for the deposits obtained under the studied conditions were around 100 HV, figure 7, figure 8. The study shows that a high degree of brightness is favoured by high current density (i = 16 mA·cm^{-2}, T = 50°C, pH = 8, without agitation), an average temperature (i = 10 mA·cm^{-2}, T = 50°C, pH = 8, without stirring) and a basic pH (i = 10 mA·cm^{-2}, T = 50°C, pH = 9.23, without stirring), figure 9.

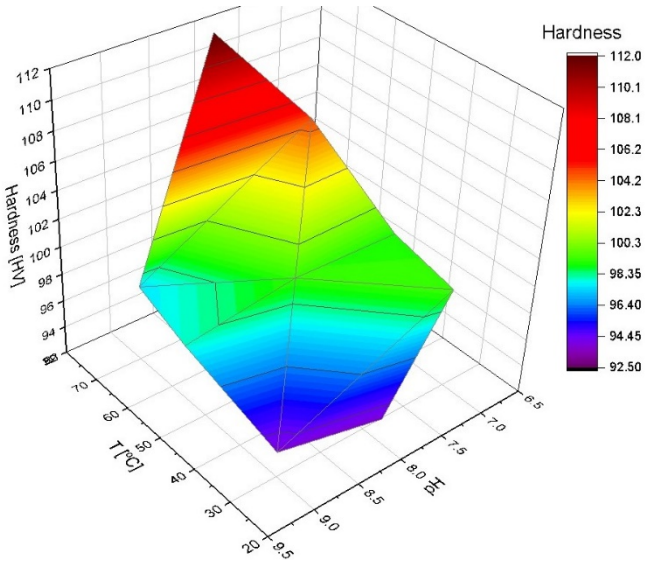


Fig. 8 − The hardness profile as a function of temperature and pH

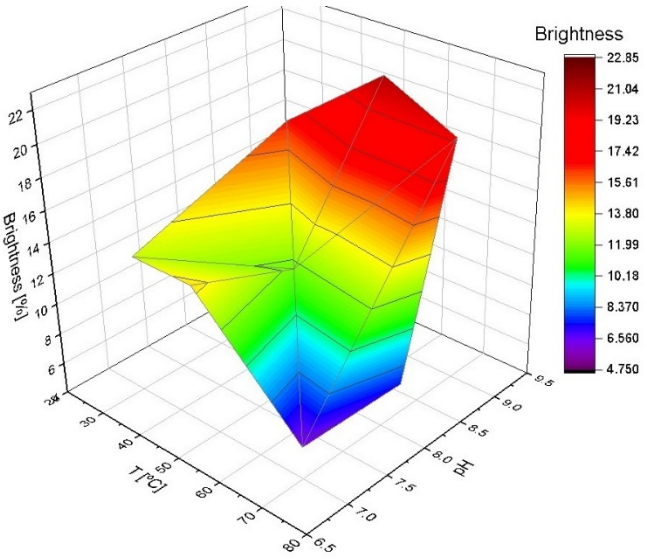


Fig. 9 − The brightness profile as a function of temperature and Ph

The brightness depends both on the surface roughness of the base metal and on the nature of the galvanic coating, therefore the roughness of the deposited galvanic layer determines the surface quality of the galvanic coatings. Thus, smoothness means both the absence of irregularities visible to the naked eye that constitute the macrogeometry of the surface, and the absence of microscopic irregularities, invisible to the naked eye, which constitutes the microgeometry of the surface. The roughness of the Ni-W alloy layers obtained at various parameters was estimated according to two coefficients: Sa - the arithmetic mean of the absolute departures of the roughness profile from the mean line throughout the sampling length and Sq - the root mean square deviation of the assessed profile. From the images presented in figures 10 - 12, it appears that NiW electrodeposition on copper substrates obtained at i = 10.00 $mA \cdot cm^{-2}$, T = 25.5°C, pH = 8 is a layer with uniform surface microgeometry. We must mention that the roughness is significantly influenced by the composition and concentration of the electrodeposition baths, by the thickness of the layer and last but not least by the composition of the alloy in the deposited layer.

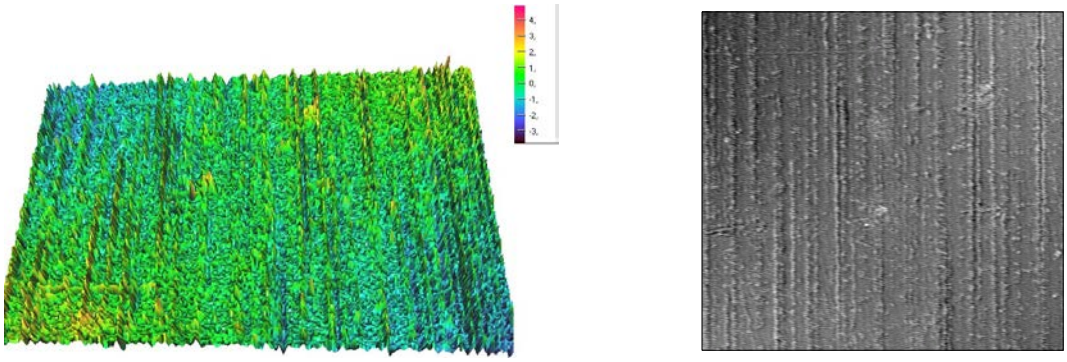


Fig. 10 − Images obtained with profilometer of NiW electrodeposition on copper substrate obtained at i = 15.00 mA·cm^{-2}, T = 30 °C, pH = 7 (no sample 2) (1 mm x 1 mm, at a resolution of 2 µm x 2 µm)

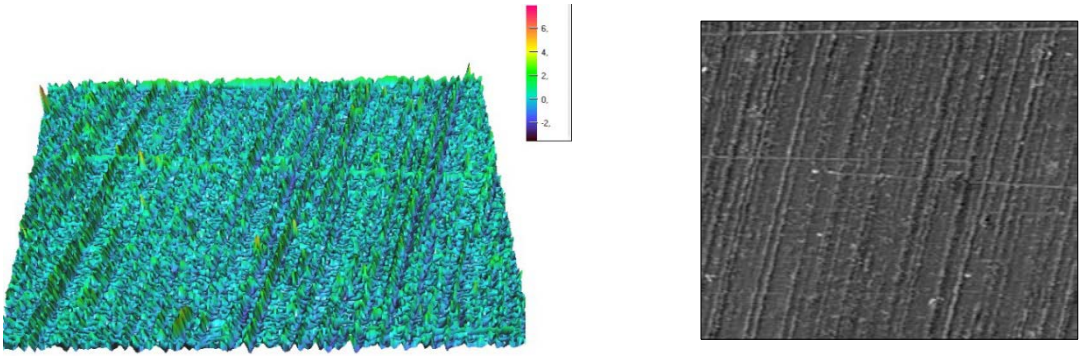


Fig. 11 − Images obtained with profilometer of NiW electrodeposition on copper substrate obtained at i = 5.00 mA·cm^{-2}, T = 70 °C, pH = 9 (no sample 7) (1 mm x 1 mm, at a resolution of 2 µm x 2 µm)

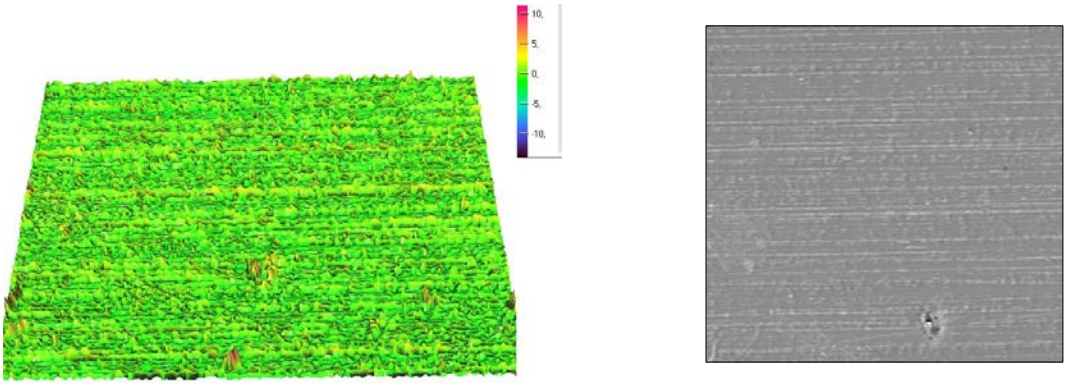


Fig. 12 − Images obtained with profilometer of NiW electrodeposition on copper substrate obtained at i = 10.00 mA·cm^{-2}, T = 25.5°C, pH = 8 (no sample 12) (1 mm x 1 mm, at a resolution of 2 µm x 2 µm)

3. Conclusions

The current efficiency decreases with an increased applied current density, and the tungsten content remains constant at around 11% for different current densities (10 mA·cm^{-2} and 16 mA·cm^{-2}, respectively). The great amount of hydrogen generated during electrodeposition causes a decrease in tungsten content and prevents further tungsten inclusion. At higher current density, the current efficiency is lower, and the hydrogen evolution is intensified, causing a supplementary agitation to the solution. All these results indicate some mass transport limitations. An increase in the temperature of the electrolyte leads to the inclusion of more tungsten. The higher temperature facilitates tungsten deposition because it increases the free convection of the electrolyte, favoring transport to the cathodic surface. The deposition rate increases with the rise of temperature in the 50 – 74.5°C range.

Deposit tungsten content and current efficiency are directly related to pH. The pH value rises from 6.78 to 8 will increase the W content from 13.51% to 14.65% and a higher current efficiency. However, a farther pH increase, from 8 to 9.23, causes a decrease in current efficiency and W content. The pH rises alter the solution equilibrium affecting the electrodeposition reactions and the deposit morphology and composition.The electrodeposition parameters influence the final properties of the alloys, such as: the layer thickness, the hardness, and the structures. The optimal deposit thickness was achieved when the following electrodeposition conditions were used: i = 10 $mA \cdot cm^{-2}$, T = 50°C, pH = 8. The deposit hardness is directly related to the alloy composition, deposit morphology, and plated layer thickness. Higher hardness, approximately 100 HV were measured. The composition and quality of the deposit can be controlled by carefully tracking the established technological parameters.

REFERENCES

[1] Haj – Taieb M., Haseeb A.S.M.A., Caulfield J., Bade K., Aktaa J., Hemker K.J., Thermal stability of electrodeposited LIGA Ni-W alloys for high-temperature MEMS applications, Microsyst. Technol., 14(2008), 1531 – 1536;

[2] Jung H., Hong C., Ki J., Kim J., Kim B., Tak Y., Pulse electrodeposition of Ni-W alloy for trench filling in microelectromechanical systems, J. Nanosci. Nanotechnol., 8(2008), 5321 – 5325;

[3] Wang H., Ding G.F., Zhao X.L., Yao J.Y., Zhu J., Wang Z.M., Fabrication of low stress Ni-W nanocristalline for MEMS devices, Shanghai JiaotongDaxueXuebao/J. Shanghai Jiaotong Univ. 41(2007), 12 – 15;

[4] Wang H., Liu R., Cheng F.J., Cao Y., Ding G.F., Zhao X.L., Electrodepositing amorphous Ni-W alloys for MEMS, Microelectron. Eng., 87(2010), 1901 – 1906;

[5] Armstrong D., Haseeb A., Wilkinson A., Roberts S., Micro-fracture testing of Ni-W microbeams produced by electrodeposition and FIB machining, MRS Proceedings, Cambridge Univ. Press, 2006 (pp. 0983-LL0908-0907);

[6] Younes O., Gileadi E., Electroplating of Ni/W Alloys (I): Ammoniacal citrate baths. J Electrochem Soc [Internet]. 2002; 149(2):C100; Available from: http://dx.doi.org/10.1149/1.1433750;

[7] Younes O., Gileadi E., Younes O. Electroplating of High Tungsten Content Ni/W Alloys. Electrochem Solid-state Lett [Internet]. 1999; 3(12): 543; Available from: https://doi.org/10.1149/1.1391203;

[8] Younes O., Zhu L., Rosenberg Y., Shacham-Diamand Y., Gileadi E. Electroplating of Amorphous Thin Films of Tungsten/Nickel Alloys. Langmuir [Internet]. 2001 Dec 1;17(26):8270–5; Available from: https://doi.org/10.1021/la010660x;

[9] Yin K.-M., Lin B.-T., Effects of boric acid on the electrodeposition of iron, nickel and iron-nickel. Surf Coatings Technology. 1996; 78(1–3): 205–10;

[10] Schloßmacher P., Yamasaki T., Structural Analysis of Electroplated Amorphous-Nanocrystalline Ni-W. Microchim Acta [Internet]. 2000 Apr 1;132(2):309–13; Available from: https://doi.org/10.1007/s006040050074;

[11] Namburi L., Electrodeposition of NiW alloys into deep recesses.pdf. 2001;

[12] Yao S., Zhao S., Guo H., Kowaka M., New Amorphous Alloy Deposit with High Corrosion Resistance. Corossion. 1996; 52(03), 183;

[13] Atanassov N, Gencheva K, Bratoeva M. Properties of nickel-tungsten alloys electrodeposited from sulfamate electrolyte. Plating and surface finishing, 1997; 84(2): 67–74;

[14] Metikos – Hukovic M., Grubac Z., Radic N., Tonejc A., Sputter deposited Nanocrystalline Ni and Ni-W films as catalysts for hydrogen evolution, J. Mol. Catal. A Chem., 249 (2006), 172 – 180;

[15] Kawashima A., Akiyama E., Habazaki H., Hashimoto K., Caracterization of sputter-deposited Ni-Mo and Ni-W alloy electrocatalysts for hydrogen evolution in alkaline solution, Mater. Sci. Eng. A 226 (1997), 905 – 909;

[16] Tasic G.S., Lacnjevac U., Tasic M.M., Kaninski M.M., Nikolic V.M., Zugic D.L., Jovic V.D., Influence of electrodeposition parameters of Ni-W on Ni cathode for alkaline water electrolyser, Int. J. Hydrog. Energy 38 (2013), 4291 – 4297;

[17] Gonzalez – Buch C., Herraiz-Cardona I., Ortega E.M., Garcia – Anton J., Perez-Herranz, Development of Ni-Mo, Ni-W and Ni-Co macroporous materials for hydrogen evolution reaction, Chem. Eng. Trans., (2013), 865 – 870;

[18] Sizova I., Kulikov A., Onishchenko M., Serdyukov S., Maksimov A., Synthesis of nickel-tungsten sulfidehydrodearomatization catalysts by the decomposition of oil-soluble precursors, Pet. Chem, 56 (2016), 44 – 50;

[19] Quiroga Arganaraz M.P., Ribotta S.B., Folquer M.E., Benitez G., Rubert A., Gassa L.M., Vela M.E., Salvarezza R.C., The electrochemistry of nanostructured Ni-W alloys, J. Solid State Electrochem. 17 (2013), 307 – 313;

[20] Rashkov R., Atanassov N., Jannakoudakis A., Jannakoudakis P., Theodoridou E., Structure and electrocatalytic activity of Ni-W thin films deposited on carbon fiber supports, J. Electrochem. Soc., 153 (2006), C152 – C156;

[21] Elias I., Hegde A.C., Electrodeposition and electrocatalytic study of Ni-W alloy coating, Mater. Sci. Forum, Trans Tech Publ 2015, pp.651 – 654;

[22] Fan C., Piron D., Sleb A, Paradis P., Study of electrodeposited nickel-molybdenum, nickel-tungsten, cobalt-molybdenum and cobalt-tungsten as hydrogen electrodes in alkaline water electrolysis, J. Electrochem. Soc., (1994), 382 – 387;

[23] Maksic A.D., Miulovic S.M., Nikolic V.M., Perovic I.M., Kaninski M.P.M., Energy consumption of the electrolytic hydrogen production using Ni-W based activators – Part I, Appl. Catal. A Gen., 405 (2011), 25 – 28;

[24] Hong S.H., Ahn S.H., Choi J., Kim H.Y., Kim H.-J., Jang J.H., Kim H., Kim S.-K., High-activity electrodeposited NiW catalysts for hydrogrn evolution in alkaline water electrolysis, Appl. Surf. Sci. (2015);

[25] Kaninski M.P.M., Saponjic D.P., Perovic I.M., Maksic A.D., Nikolic V.M., Electrochemical characterization of the Ni-W catalyst formed in situ during alkaline electrolityc hydrogen production – Part II, Appl. Catal. A Gen., 405 (2011), 29 – 35;

[26] Guo Z, Zhu X, Zhai D, Yang X. Electrodeposition of Ni-W amorphous alloy and Ni-W-SiC composite deposits, 材料科学技术 (英文版), 2000;

[27] Poroch – Seriţan M., Cercetăriprivindcontrolulîntimp real, prinspectroscopie, al băilorgalvanice de nichelare, (PhD Thesis) Suceava, 2010;

[28] Poroch – Seriţan M., Gutt G., Severin T., Bobu M., Influence of pH galvanic baths on the nickel deposits. Annals of Dunărea de Jos University of Galaţi, Fascicle IX Metallurgy and Materials Science, 2009; 2: 315 – 320;

[29] Dias A., Ciminelli V.N.S., Thermodynamic calculation and modeling of the hydrothermal synthesisi of nickel tungstates, J. Eur. Ceram. Soc. 21 (2001), 2061 – 2065;

[30] Sen A., Pramanik P., A chemical syntetic route for the preparation of fine-grained metal tungstate powders (M = Ca, Co, Ni, Cu, Zn), J. Eur. Ceram. Soc. 21 (2001), 745-750;

[31] Amadeh A., Harsijsani M., Moradi H., Wear behavior of carbon steel electrodeposited by nanocrystalline Ni-W coatings, Int. J. ISSI 6 (2009), 14 – 19;

[32] Obradovic M.D., Bosnjakov G.Z, Stevanovic R.M., Maksimovic M.D., Despic A.R., Pulse and direct current plating of Ni-W alloys from ammonia-citrate electrolyte, Sulf. Coat. Technol., 200 (2006), 4201 – 4207;

[33] Oue S., Nakano H., Kobayashi S., Fukushima H., Structure and codepositionbehavior of Ni-W alloys electrodeposited from ammoniacal citrate solutions, J. Electrochem Soc. 156 (2009) D17-D22;

[34] Zemanova M., Kurinec R., Jorik V., Kadleciova M., Ni-W alloy coating deposited from a citrate electrolyte, Chem. Pap. 66 (2012), 492 – 501;

[35] Wang Y., Zhou Q., Li K., Zhong Q., Bui Q.B., Preparation of Ni-W-SiO2 nanocomposite coating and evaluation of its hardness and corrosion resistance, Ceram. Int. 41 (2015), 79 – 84;

[36] Bratoeva M., Atanasov N., Effect of sulfamate-citrate electrolyte pH on the Ni-W alloy electrodeposition, Russ. J. Electrochem. 36 (2000), 60 – 63;

[37] Bera P., Kumar M.D., Anandan C., Shivakumara C., Characterization and microhardness of electrodeposited Ni-W coatings obtained from gluconate bath, Surf. Rev. Lett. (2014);

[38] Mizushima I., Tang P.T., Hasen H.N., Somers M.A.J., Development of a new electroplating process for Ni-W alloy deposits, Electrochim. Acta 51 (2005), 888 – 896;

[39] Mizushima I., Tang P.T., Hasen H.N., Somers M.A.J., Identification of an anomalous phase in Ni-W electrodeposits, Surf. Coat. Technol. 202 (2008) 3341 – 3345;

[40] Mizushima I., Electrodeposition of Ni-W Alloy and Characterization of Microstructure and Properties of the Deposits (PhD Thesis) 2006;
[41] Brenner A., Electrodeposition of Alloys, Academic Press Inc., New York, 1963;
[42] Holt M., Vaaler L., Electrolytic reduction of aqueus tungstate solutions, J. Electrochem. Soc. 94 (1948), 50 – 58;
[43] Clark W.E., Lietzke M., The mechanism of the tungsten alloy plating process. J. Electrochem Soc. 99 (1952), 245 – 249;
[44] Fukushima H., Akiyama T., Akagi S., Higashi K., Role of iron-group metals in the induced codeposition of molybdenum from aqueous solution, Trans. Jpn. Inst. Metals 20 (1979), 358 – 364;
[45] Podlaha E., Landolt D., Induced codeposition II. A mathematical model describing the electrodeposition of Ni-Mo alloys, J. Electrochem. Soc. 143 (1996), 893 – 899;
[46] Podlaha E., Landolt D., Induced codeposition III. Molybdenum alloys with nickel, cobalt and iron, J. Electrochem. Soc. 144 (1997), 1672 – 1680;
[47] Niu Z.-J., Yao S.-B., Zhou S.-M., In situ surface Raman investigation on induced codeposition of an Fei-Mo alloy, J. Electroanal. Chem. 455 (1998), 205 - 207;
[48] Zeng Y., Li Z., Ma M., Zhou S., In situ surface Raman study of the induced codeposition mechanism of Ni-Mo alloys, Electrochem. Commun. 2 (2000), 36 – 38;
[49] Obradovic M., Stevanovic R., Despic A., Electrochemical deposition of Ni-W alloys from ammonia-citrate electrolyte, J. Electroanal. Chem. 552 (2003), 185 – 196;
[50] Kabi S., Raeissi K., Saatchi A., Effect of polarization type on properties of Ni-W nanocrystalline electrodeposits, J. Apple. Electrochem. 39 (2009), 1279 – 1285;
[51] Eliaz N., Gileadi E., The mechanism of induced codeposition of Ni-W alloys, ECS Trans., (2007), 337 – 349;
[52] Eliaz N., Gileadi E., Induced codeposition of alloys of tungsten, molybdenum nd rhenium with transition metals, Modern Aspects of Electrochemistry, Springer 2008, pp. 191 – 301;
[[53] Ibrahim M.A.M., Rehim S.S.A.E., Wahaab S.M. A.E., Dankeria M.M., Nickel Electroplating On Steel From Acidic Citrate Baths. Plat Surf Finish. 1999 aprilie. 69-74, https://www.nmfrc.org/pdf/p0499i.pdf;
[54] Moussa S., Ibrahim M., Rehim S.A.E., Induced electrodeposition of tungsten with nickel from acidic citrate electrolyte. Journal of applied electrochemistry. 2006; 36(3): 333–8;
[55] Yamasaki T, High-strength nanocrystalline Ni-W alloys produced by electrodeposition and their embrittlement behaviors during grain growth. Scripta Materialia. 2001 May; 44(8–9):1497; DOI:10.1016/S1359-6462(01)00720-5;
[56] Nasu T., Sakurai M., Kamiyama T., Usuki T., Uemura O., Yamasaki T. EXAFS study on amorphous and nanocrystalline M–W (M = Fe; Ni) alloys produced by electrodeposition Journal of Non-Crystalline Solids. 2002; 312-314; 319–322;
[57] Omi T., Glass H., Yamamoto H., Phase Structure and Composition of Fe-W Alloy Electrodeposits. Journal of the Electrochemical Society. 1976; 123(3):341.